

# Model-Based State Recognition of Bone Drilling with Robotic Orthopedic Surgery System

Haiyang Jin, Ying Hu\*, Zhen Deng, Peng Zhang, Zhangjun Song and Jianwei Zhang

**Abstract**—Screw path drilling is an important process among many orthopedic surgeries. To guarantee the safety and correctness of this process, a model-based drilling state recognition method is proposed in this paper. The thrust force in the drilling process is modeled based on an accurate 3D bone model restructured by means of Micro-CT images. In theoretical modeling of the thrust force, the resistance and the elasticity of the bone tissues are considered. The cutting energy and elastic modulus are defined as the material parameters in the theoretical model, which are identified via a least square method. Some key parameters are proposed to support the state recognition: the peak forces in the first and the second cortical layers, the average force in the cancellous layer and the thickness of each layer. Based on these key parameters in the model, a state recognition strategy with a robotic orthopedic surgery system is proposed to recognize the switch position of each layer. Experiments are performed to demonstrate the effectiveness of the modeling approach and the state recognition method.

**Keywords**—orthopedic surgery; Micro-CT; bone drilling; state recognition

## I. INTRODUCTION

In many orthopedic surgeries, bone drilling is one of the most important procedures for inserting bone screws [1]. As many important vessels and nerves surround the bones, incorrect screw path drilling may cause patients irreparable damage. Using a robotic surgery system to perform this drilling process can help surgeons to improve their accuracy and lower the risk.

The requirements of bone drilling are different in different surgeries. For example, in operations with interlocking intramedullary nailing, the screw path crosses the entire bone layers [2]; while in transpedicular fixation operations, the screw path stops at the second cortical layer of the vertebral bone [3]. Therefore, to recognize the drilling state in the bone drilling process, real-time thrust force feedback is being used in robotic systems by many scholars.

\*This research supported by the National Natural Science Foundation of China (No.61175124 and No.51005227), Key Research Program of the Chinese Academy of Sciences (No.KJZD-EW-TZ-L03) and Guangdong Innovative Research Team Program (No. 201001D0104648280).

Haiyang Jin is with Harbin Institutes of Technology Shenzhen Graduate School, Guangdong Provincial Key Laboratory of Robotics and Intelligent System, Shenzhen Institutes of Advanced Technology, Chinese Academy of Sciences, The Chinese University of Hong Kong (hy.jin@siat.ac.cn)

Ying Hu\*(corresponding author), Zhen Deng, Peng Zhang and Zhangjun Song are with Guangdong Provincial Key Laboratory of Robotics and Intelligent System, Shenzhen Institutes of Advanced Technology, Chinese Academy of Sciences, The Chinese University of Hong Kong (ying.hu@siat.ac.cn, zhen.deng@siat.ac.cn, zhangpeng@siat.ac.cn and zj.song@siat.ac.cn)

Jianwei Zhang is with University of Hamburg, Germany (zhang@informatik.uni-hamburg.de)

Most existing studies in drilling state recognition focus on a general model of the drilling thrust force, which is obtained via an analysis of a large number of experiments. Examples of this are the bone drilling systems developed by Bouazza-Marouf and Ong from Loughborough University (UK)[4], Louredo et al. from the University of Navarra (Spain) [5], Lee et al. from Lunghwa University of Science and Technology (Taiwan) [6], etc. However, these kinds of drilling state recognition are not aimed at each single screw path. In current clinical manual operation, surgeons will estimate the depth of the planned screw path. This estimation provides a previous prediction for drilling processes. Based on this idea, Wang et al. from Beihang University (China) developed a 3D navigation and monitoring system for spinal milling operation based on the registration between multi-planar uoroscopy and CT images [7]. We have proposed an image-force fusion method for state recognition in previous research [8]. However, the model in the approach is based on normal CT or MR images, which can only provide the shape of the bone without the inner microstructure of the bone. That causes the low recognition rate between the cortical and cancellous layers in the bone. An accurate 3D model of the bone can help to improve the drilling state recognition.

For modeling the relationship between the 3D model of the bone and operation force feedback of the drilling process, a number of approaches for bone modeling have been presented [9-11]. Agus et al. [9] propose a patient-specific volumetric object model to represent the bone, and the thrust force is presented based on the Hertz contact theory. Petersik et al. [10] represent a bone model by volumetric pixels (voxels), and the spherical drill bit is illustrated by an array of sample points that cover its surface. A multi-point collision detection approach is introduced in their research. Mohammadreza et al. [11] present a voxel representation of the virtual bone, and the drill bits are modeled as a set of small chips with an estimated thickness and known material stiffness. The total force is calculated by integrating all forces over all thrust chips. These volume-based or voxel-based methods are all built on graphic simplification of the real structure of bones, and they can hardly show the complex microscopic bone structures. However, the mechanical characteristics of the bone are significantly influenced by the inner microstructure.

Considering the above challenges, in this paper, a new method for modeling thrust force of bone drilling is proposed based on an accurate 3D point cloud model. The 3D point cloud model is gained by Micro-CT scanning so that the inner microstructure of the bone remains. For modeling the theoretical thrust force, resistance and elasticity issues

are considered. Furthermore, a model based drilling state recognition algorithm is proposed. The key parameters in the pre-operative model simulation are used in the intra-operative state recognition. The experiments to demonstrate the effectiveness of the modeling method and the recognition algorithm are performed on a piece of lamellar pig bone.

The rest of the paper is organized as follows. In section II, the model of the thrust force in the drilling process is described. The model based drilling state recognition algorithm is represented in section III. Section IV gives some verifying experiments, and conclusions are summarized in section V.

## II. DRILLING PROCESS MODELING

### A. Description of Drilling Process

In bone screw insertion operations, the most important process is screw path drilling in that the screw path determines the position, orientation and depth of screw insertion. Fig. 1 shows a Micro-CT scan of a typical bone structure. Two layers of cortical tissues cover the surface of the bone and cancellous tissue is inside. In some operations, the screw path crosses all these three layers and penetrates through the bone. In other conditions, like e.g. spinal surgeries, the path should end nearby the second cortical layer. The control of the depth in these cases is a challenge in clinical operations. However, the real-time thrust force performs differently in cortical and cancellous layers due to their different microscopic structures, and can be used to recognize the different states in the drilling process to check the correctness of the screw path.

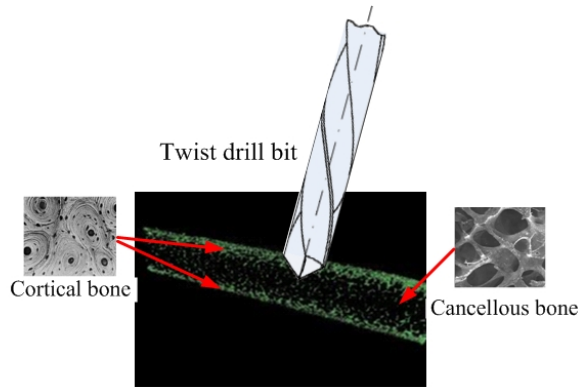


Fig. 1. Bone drilling process

### B. Bone Modeling via Micro-CT Images

The traditional modeling method using CT scanning can only achieve a surface or a solid model of the bone. The microscopic structures of the cortical and cancellous bone are hardly present in the model [12, 13]. For bone drilling process modeling, in this paper, a 3D model of the bone is obtained via Micro-CT images to attain the accurate structure of the bone. The 3D point-cloud model is restructured via the arrays of Micro-CT images. Through this process, the microstructure of the cortical bone and the cancellous bone is

illustrated by the distribution of the points. The point density is higher in the cortical layer and lower in the cancellous bone.

### C. Theoretical Modeling of Thrust Force

In the drilling process, two components influence the thrust force  $F_t$  of screw path drilling: resistance generated by the machining process, and elasticity from the elastic deforming of the test bone. Equation (1) illustrates the thrust force with the two effects, where  $F_c$  and  $F_e$  respectively present the resistant and elastic components of the thrust force, and  $a \in (0,1)$  is the parameter to manage their ratio.

$$F_t = aF_c + (1 - a)F_e \quad (1)$$

The resistance is influenced by the geometric shape of the drill bit, the feed speed and the material parameters of the bone [14]. The first two influencing components are easy to attain: the diameter and vertex angle of the drill bit are standard, and the feed speed is previously set. However, the material parameters are hard to acquire. To simplify the modeling process, the cutting energy, which can be gained through experiments in a certain rotational speed, is used to represent the influence of the material parameters. As shown in Fig. 2, when the drill bit gets into contact with the 3D model of the vertebra, the cutting force is generated by (2).

$$F_c = \frac{1}{2}N \cdot K \cdot D \cdot \sin\left(\frac{\beta}{2}\right) \quad (2)$$

where  $N$  is the number of the points removed in one simulation step;  $D$  is the diameter of the drill bit;  $\beta$  is the vertex angle and  $K$  is the total energy of per unit volume required to cut the material.

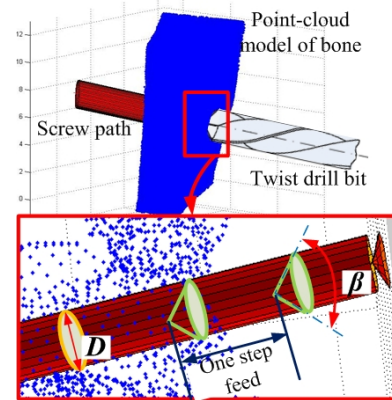


Fig. 2. Drill bit penetrates 3D point-cloud model

The elastic component of the drilling bone is modeled by the Hertz contact theory. The drilling process with the twist drill can be abstracted as a solid cone pressing and deforming an elastic material, and the elastic component of the thrust force is also determined by the feed speed, geometry and the material parameters [15, 16].

$$F_e = \frac{\pi}{2}E \cdot d^2 \cdot \tan\left(\frac{\beta}{2}\right) \quad (3)$$

where  $E$  presents the elastic modulus;  $d$  is the depth of the indentation;  $D$  is the diameter of the drill bit;  $\beta$  is the vertex angle of the bit. The drilling process of the elastic component can be shown in Fig. 3.

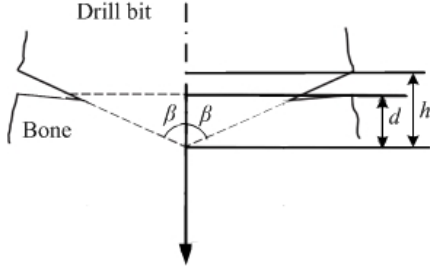


Fig. 3. Model of elastic component of thrust force

where  $d$  is the depth of the drill bit penetrating in the bone, and  $h$  is the height of the tip of the drill bit.

#### D. Parameter Identification

The material parameters, cutting energy  $K$  and elastic modulus  $E$  are determined by means of the microstructure and density of the bone. They feature different properties in different layers of the bone. To simplify the modeling process, the material parameters are sectionally identified in each bone layer.  $K = K_{p1}$ ,  $K_s$  or  $K_{p2}$  represent the cutting energy in the first cortical layer, the cancellous layer and the second cortical layer. As the elastic deformation of the bone is mainly generated in the cortical layers, the elastic component is considered only in the cortical layers and  $E = E_{p1}$  or  $E_{p2}$  represent the elastic modulus in the first and the second cortical layers.

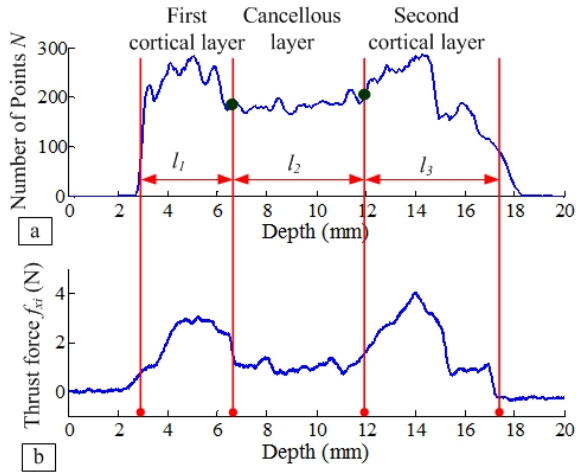


Fig. 4. Boundary detection between different materials; (a) Distribution of points along screw path; (b) Actual thrust force measurement

The bone layers are separated by means of the distribution of the point-cloud in different layers of the bone. The density of the point-cloud in the cortical bone is higher than that in the cancellous bone so that the cortical bone and the cancellous bone can be distinguished by the point-cloud

distribution along the screw path. The approach for obtaining distribution along certain screw path is introduced in [8]. The boundaries of each bone layer are detected with point-cloud density thresholds. Fig. 4a shows the point distribution on one screw path. Positions of the boundaries are recorded and the thickness of each layer can be calculated.

The experiments with the same screw path planned in the 3D bone model are performed to gain the actual thrust force in the real drilling process, as shown in Fig. 4b. The least squares method is used to solve the parameter identification, as shown in (4).

$$\min ES(K, E)$$

$$\begin{cases} ES(K_{p1}, E_{p1}) = \sum_{i=0}^{l_1} (F_t(N(x_i), d(x_i)) - f_{xi})^2 \\ ES(K_s) = \sum_{i=0}^{l_2} (F_t(N(x_i), d(x_i)) - f_{xi})^2 \\ ES(K_{p2}, E_{p2}) = \sum_{i=0}^{l_3} (F_t(N(x_i), d(x_i)) - f_{xi})^2 \end{cases} \quad (4)$$

where the  $ES(K, E)$  represents the error sums of squares between theoretical and actual forces in three layers; the  $x_i$  is the depth in each layer;  $l_1$ ,  $l_2$  and  $l_3$  are the thicknesses of each layer;  $f_{xi}$  is the actual thrust force related to the current depth  $x_i$ . The  $N(x_i)$  presents the numbers of points in the 3D model related to current depth  $x_i$ ; and  $d(x_i)$  is the indentation depth shown in (5).

$$d = \begin{cases} x_i & x_i \leq h \\ h & x_i > h \end{cases} \quad (5)$$

where  $h$  is the height of the drill bit, as shown in Fig. 3.

Based on the above-mentioned parameter identification method, a group of experiments are carried out on the lamellar bone of a pig to gain its average material parameters:  $K_{p1} = 0.0049$ ,  $K_s = 0.0035$ ,  $K_{p2} = 0.0043$ ,  $E_{p1} = 0.1185$  and  $E_{p2} = 0.3424$ .

### III. STATE RECOGNITION STRATEGY

#### A. Key Parameters of the Simulation Force

To apply the simulation results to the state recognition, some key parameters of the simulation thrust force are proposed. Fig. 5 shows the simulation results of the thrust force and the related key parameters, including the peak thrust force  $f_{peak1}$  and  $f_{peak2}$  in the first and second cortical layers, the average thrust force  $f_s$  in the cancellous layer and the thicknesses  $h_{p1}$ ,  $h_{p2}$  and  $h_s$  of each layer.

The key force values  $f_{peak1}$ ,  $f_{peak2}$  and  $f_s$  are used for recognizing the different states, and the thickness parameters  $h_{p1}$ ,  $h_{p2}$  and  $h_s$  are used to estimate the accuracy of the model of the thrust force.

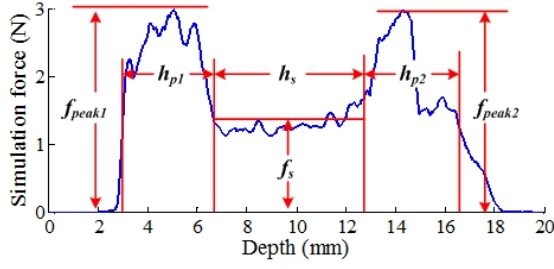


Fig. 5. Result of simulation force and key parameters

### B. State Recognition Strategy

In order to guarantee the safety and correctness of the drilling process, the appropriate depth of the screw path must be carefully determined. In our previous research with the robotic orthopedic surgery system, an experiment-based drilling state recognition algorithm was proposed to control the depth of the screw path [17]. However, this previous work on controlling the depth of the screw path is not aimed at each planned screw path. Based on the aforementioned model simulation and related key parameters, the drilling states of different screw paths can be recognized in real-time. The state recognition algorithm is described in Fig. 6. The symbols in the following flowchart are described as:

$s_{cur}$  — the current state;  $s_{cur} = 1, 2, 3, 4$  or  $5$  represent the non-contact state, the first cortical state, the cancellous state, the second cortical state and the penetrated state, respectively.

$P_{cur}$  — the current depth of the screw path.

$f_{cur}$  — the current thrust force.

$f_{th1}, f_{th2}, f_{th3}$  and  $f_{th4}$  — the thresholds of drilling state recognition.

$P_{s2}, P_{s3}, P_{s4}$  and  $P_{s5}$  — the switch positions of state 2, 3, 4 and 5.

$f_{peak1}, f_{peak2}, f_s, h_{p1}, h_s$  and  $h_{p2}$  are the aforementioned key parameters. In the algorithm, the switch positions  $P_{s2}, P_{s3}, P_{s4}$  and  $P_{s5}$  are recognized via thresholds as shown in (6).

$$\begin{cases} f_{th1} = f_s \\ f_{th2} = f_s + (f_{peak1} - f_s) \cdot k_1 \\ f_{th3} = f_s + (f_{peak2} - f_s) \cdot k_2 \\ f_{th4} = f_s \end{cases} \quad (6)$$

where the  $k_1$  and  $k_2$  are the ratio coefficients for adjusting the threshold of state 3 and state 4. The thresholds are based on the peak forces  $f_{peak1}$  and  $f_{peak2}$  in the cortical layers and average force  $f_s$  in the cancellous layers in the previous model simulation. For eliminating the effects of signal fluctuation, a short time delay is performed near the switch positions  $P_{s2}, P_{s3}$  and  $P_{s4}$ . Meanwhile, the switch positions and the thickness of the cortical and cancellous layers are recorded to identify the accuracy of the model simulation.

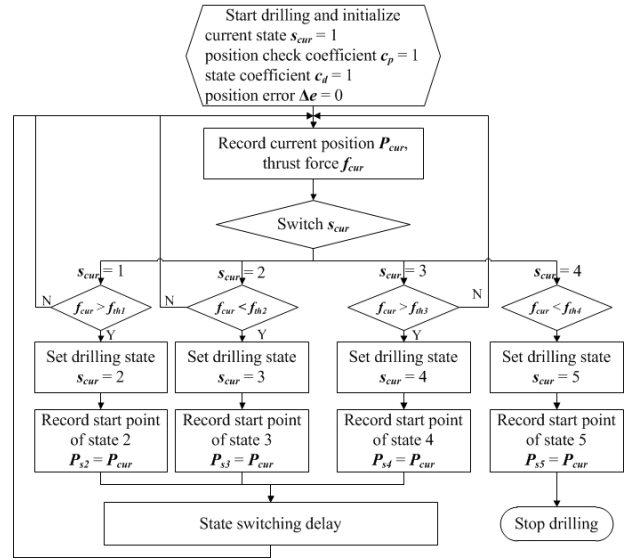


Fig. 6. Flowchart of the state recognition

## IV. EXPERIMENTS AND DISCUSSIONS

### A. System Description

The experiment system for the model-based drilling state recognition with a robotic orthopedic surgery system is shown in Fig. 7, which includes four main hardware and software modules: the pre-operative modeling module; the simulation module, the robotic orthopedic surgery system and the state recognition module.

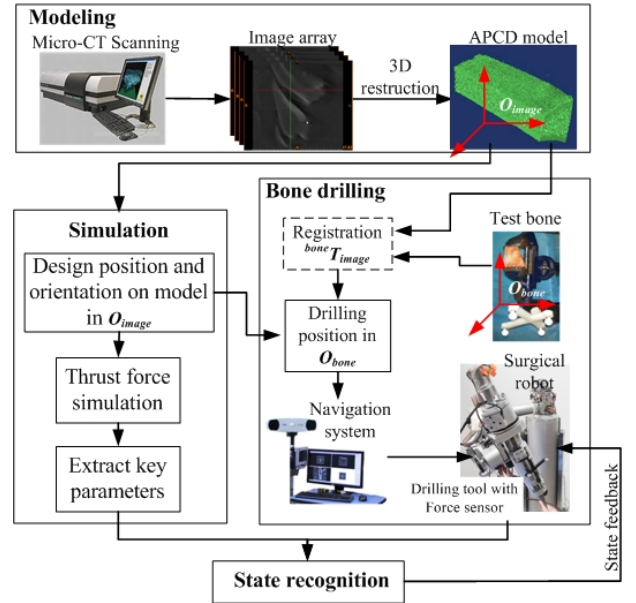


Fig. 7. System structure of model-based state recognition

In the 3D modeling module, a Micro-CT is used to scan and gain an array of images of the test bone. And a 3D model in the image coordinate frame  $O_{image}$  is obtained by 3D reconstruction process. The test sample in the experiments is a piece of the lamellar bone of a pig. For different screw paths



on the bone, the thickness of the test bone is different, as shown in Fig. 8a. Fig. 8b is one of the Micro-CT images, and Fig. 8c shows the restructured 3D model.

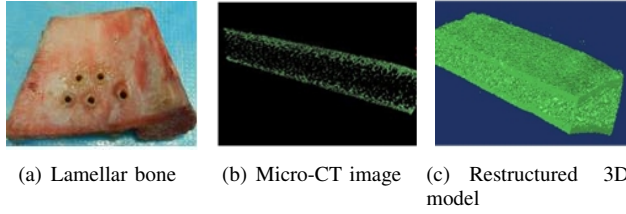


Fig. 8. Images in different stages

In the simulation process, the prepared 3D model is imported in the simulation module. The surgeon first designs the screw path in the image coordinate frame  $O_{image}$ , and then performs the simulation of the thrust force in the drilling process along the planned screw path. The model of the thrust force in the entire drilling process is recorded, and the key parameters are extracted.

The intra-operative drilling process is carried out by a surgical robot, which consists of a 6 Degree-of-Freedom (DoF) surgical robot, a drilling tool with a force sensor, and a navigation system with a tracking device. The navigation system tracks and navigates the surgical robot positioning on the test bone. The navigation information is in the bone coordinate frame  $O_{bone}$ . In the bone drilling process, the navigation information is gained via the planning screw path in  $O_{image}$ , therefore, a transformation matrix  ${}^{bone}T_{image}$  between  $O_{bone}$  and  $O_{image}$  is obtained via a point-based registration. Then, the pre-planned screw path in the simulation module is transformed into the navigation path and sent to the surgical robot for positioning on the test bone. A 6-DoFs force/torque sensor is mounted on the drilling tool to sense the thrust force in real-time.

In the state recognition module, the key parameters and the real-time thrust force are imported. Based on these data, the drilling states are recognized and fed back to the surgical robot for control of the depth in the drilling screw path.

In all groups of experiments, the simulation force and the actual thrust force are all influenced by the geometrical parameters of the drill bit. A twist drill bit with diameter of  $\phi 3mm$  are chosen. The feed speed is  $0.5mm/s$  and rotational speed is  $8000rpm$ .

### B. Modeling experiments

To demonstrate the effectiveness of the modeling approach, comparative experiments are carried out. A screw path is designed in a model simulation. With the navigation system, the robot moves and positions the drilling tool on the planned screw path. The entire screw path, penetrating the lamellar bone, is drilled and the thrust force during this process is sensed. By comparing the simulation and experimental force and thickness of layers, the correctness of the 3D model can be verified. Fig. 9 shows two groups of comparison experiments on different screw paths. The upper figures show the model based simulation results of the path

and the related key parameters. The results of the real drilling process are shown in the lower figures. The states 1, 2, 3, 4 and 5 are well recognized, and the related parameters are obtained.

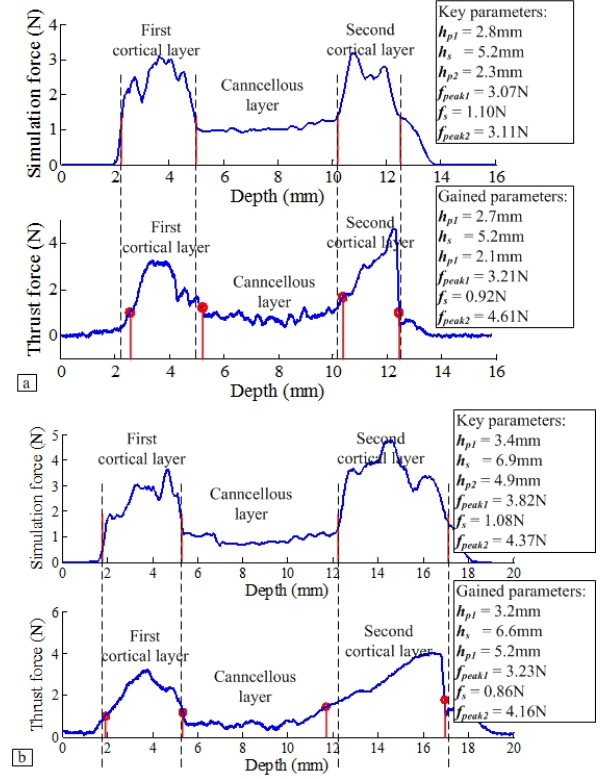


Fig. 9. Two groups of comparison results of modeling experiments

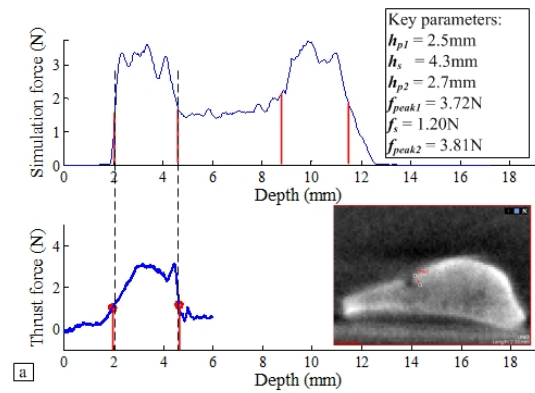
From the figures, to evaluate the precision of the model, the thickness errors of each layer between simulation actual thrust forces are measured and compared. The maximal thickness error in the experiments is within  $0.3mm$ . As the tolerant error of the orthopedic operation is less than  $0.5mm$ , a value which was identified through interviews with surgeons, the precision of the 3D model satisfies the operation requirements.

### C. State recognition experiments

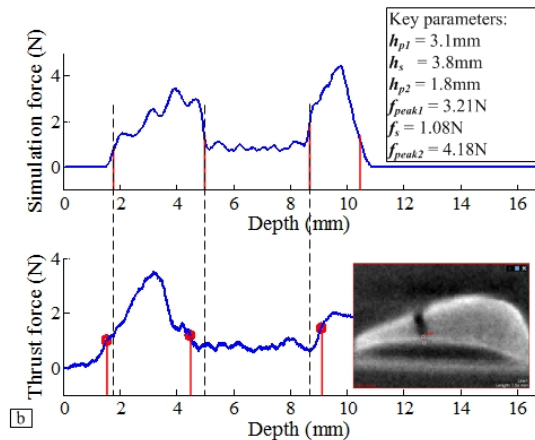
Similar to the modeling experiments, based on the previous simulation and navigation system, the drilling tool is located on the planned screw path. To verify the result of state recognition, the drilling process is stopped when the drill bit reaches the switch positions. Fig. 10a and Fig. 10b show two groups of experiments that stop at  $P_{s3}$  and  $P_{s4}$ , respectively. The X-ray images show the depth of the screw paths.

## V. CONCLUSION

In this paper, the screw path drilling process in orthopedic surgeries is focused on and a model-based drilling state recognition method is proposed. The actual bone drilling state recognition is combined with a previous model and simulation.



(a) Stopped while breaking through the first cortical layer



(b) Stopped while reaching the second cortical layer

Fig. 10. Two groups of drilling state recognition experiments

A 3D model of the bone is restructured with Micro-CT images which can illustrate the microstructure of the cortical and the cancellous bone. The issues of resistance and elasticity are considered in the theoretical modeling of the thrust force. By fitting theoretical data with trust force in practical drilling, the material parameters in the theoretical model are identified. The model of the thrust force and the related key parameters along certain screw paths can be obtained. Moreover, a state recognition algorithm based on the aforementioned model and the key parameters are proposed and realized on a robotic orthopedic surgery system. The recognition process combines the predicted results from the model based simulation and the real-time drilling.

In the test experiments for verifying the accuracy of the modeling approach, key parameters in simulation and actual drilling are compared. The results show that the trend of the thrust force and the thickness of each layer are similar along the same screw path. This demonstrates the effectiveness of the proposed modeling method. The state recognition experiments also verify that the model based recognition algorithm is available for identifying the drilling states and can be used for controlling the depth of the screw path.

Based on this work, the effectiveness of the pre-operative

planning on the 3D model can be previously predicted. And the intra-operative operation state of each single screw path can also be detected based on an individual model to improve the recognition precision.

These are some limitations in our works. For example, the scanning range of the Micro-CT used in this paper is too small to scan a living human; and the scanning time is also too long. These should be overcome in the future researches.

## REFERENCES

- [1] G.B. Chung, S.G. Lee, S. Kim, B.J. YiW. Kim, S.M. Oh, Y.S. Kim, J. Park, S.H. Oh. "A robot-assisted surgery system for spinal fusion," in Proceedings of IEEE/RSJ International Conference on Intelligent Robots and Systems (IROS 2005), 2005, Edmonton, Alberta, Canada, pp.3015-3021.
- [2] X. Duan, M. Al-Qwbani, Y. Zeng, W. Zhang and Z. Xi-ang. "Intramedullary nailing for tibial shaft fractures in adults," Cochrane Database of Systematic Reviews 2012, Issue 1. DOI: 10.1002/14651858.
- [3] L.M. Cheng, J.J. Wang, Z.L. Zeng, R. Zhu, Y. Yu, C. Li and Z.R. Wu. "Pedic screw fixation for traumatic fractures of the thoracic and lumbar spine," Cochrane Database of Systematic Reviews 2013, Issue 5. DOI: 10.1002/14651858.CD009073.
- [4] F.R. Ong and K. Bouazza-Marouf, "The detection of drill bit breakthrough for the enhancement of safety in mechatronic assisted orthopaedic drilling," *Mechatronics*, 1999, Vol. 9, pp. 565-588.
- [5] M. Louredo, I. Díaz and J.J. Gil, "DRIBON: A mechatronic bone drilling tool," *Mechatronics*, 2012, Vol. 22, pp. 1060-1066.
- [6] W.Y. Lee, C.L. Shih, S.T. Lee. "Force Control and Breakthrough Detection of a Bone-Drilling System," *IEEE/ASME Transactions on Mechatronics*, 2004, Vol.9, pp.20-29.
- [7] S. Luan, T. Wang, W. Li, Z. Liu, L. Jiang, L. Hu. "3D navigation and monitoring for spinal milling operation based on registration between multiplanar fluoroscopy and CT images," *Computer Methods and Programs in Biomedicine*, 2012, Vol. 108, pp. 151-157.
- [8] H. Jin, Y. Hu, H. Luo, T. Zheng, P. Zhang. "Intraoperative State Recognition of a Bone-Drilling System with Image-Force Fusion," in Proceedings of International Conference on Multisensor Fusion and Integration for Intelligent Systems (MFI 2012), 2012, Hamburg, Germany, pp. 275-280.
- [9] M. Agus, A. Giachetti, E. Gobbetti, G. Zanetti, A. Zorcolo. "Real-Time Haptic and Visual Simulation of Bone Dissection," *Presence: Teleoperators and Virtual Environments*, 2003, Vol.12, pp. 110-122.
- [10] A. Petersik, B. Pflesser, U. Tiede, K.H. H?hne, R. Leuwer. "Realistic Haptic Interaction in Volume Sculpting for Surgery Simulation," *Lecture Notes in Computer Science*, 2003, Vol.2673, pp 194-202.
- [11] A. Mohammadreza, M. Majid, N. Ali, M. Mohsen, R. Barry, S. Bijan. "Physics-Based Haptic Simulation of Bone Machining," *IEEE Transactions on Haptics*, 2011, No.1, Vol.4, pp.39-50.
- [12] H. Woo, E. Kang, S. Wang, K.H. Lee. "A new segmentation method for point cloud data," *International Journal of Machine Tools and Manufacture*, 2002, Vol.42, pp.167-178.
- [13] B.D Metscher. "MicroCT for comparative morphology: simple staining methods allow high-contrast 3D imaging of diverse non-mineralized animal tissues," *BMC Physiology*, 2009, Vol.9, pp.1-11.
- [14] B. Allotta, G. Giacalone, L. Rinaldi. "A Hand-Held Drilling Tool for Orthopedic Surgery," *IEEE/ASME Transactions on Mechatronics*, 1997, Vol.2, pp.218-229.
- [15] G.G. Adams, M. Nosonovsky. "Contact modeling – forces," *Tribology International*, 2000, Vol.33, pp.431-442.
- [16] Y. Lee, J. F. Hamilton, J. W. Sullivan. "The Lumped Parameter Method for Elastic Impact Problems," *Journal of Applied Mechanics*, 1983, Vol.50, No.4a, pp.823-827.
- [17] Y. Hu, H. Jin, L. Zhang, J. Zhang, P. Zhang. "State Recognition of Pedicle Drilling with Force Sensing in a Robotic Spinal Surgical System," *IEEE Transaction on Mechatronics*, DOI: 10.1109/T-MECH.2012.2237179.